

## ARTICLES

## Interaction between Polarized Triplets and Stable Radicals in Liquid Solutions

Aharon Blank and Haim Levanon\*

*Department of Physical Chemistry and the Farkas Center for Light-Induced Processes,  
The Hebrew University of Jerusalem, 91904 Israel**Received: January 4, 2001; In Final Form: February 22, 2001*

The magnetization generated by the interaction of stable radicals with photoexcited triplets in a viscous solution at room temperature was measured by light-induced Fourier transform electron paramagnetic resonance spectroscopy (FT-EPR). High and long-lived polarized magnetization ( $> 100 \mu\text{s}$  in emission) is generated in the stable radical ( $\alpha,\gamma$ -bisdiphenylene- $\beta$ -phenylallyl) interacting with the photoexcited triplet state of free base, and Zn, tetraphenylporphyrin. Radical-triplet interaction was analyzed quantitatively employing a combined model of electron spin polarization transfer (ESPT) and radical-triplet pair mechanism (RTPM). The presented model allows calculating the radical polarization following an encounter with a thermal or nonthermal triplets. Moreover, an important conclusion from this study is that the generation of radical polarization via RTPM does not require efficient quenching of the photoexcited triplet.

## I. Introduction

In solution, when photoexcited triplets interact with stable radicals, the radical's EPR spectrum changes from its normal Boltzmann spin distribution into a polarized spectrum, i.e., electron spin polarization (ESP).<sup>1-5</sup> This phenomenon was attributed to the occurrence of two complimentary mechanisms, namely electron spin polarization transfer (ESPT) and radical-triplet pair mechanism (RTPM).<sup>6</sup> The ESPT was related to the case where the triplet, which interacts with the radical, is spin polarized, whereas RTPM was attributed to a situation where the triplet levels are in thermal equilibrium.

The theoretical aspects of RTPM were treated extensively by analytical<sup>7-10</sup> and numerical<sup>5</sup> methods by solving the stochastic Liouville equation (SLE). The analysis of RTPM enables to predict the radical polarization as a function of molecular and magnetic parameters such as radical-triplet exchange interaction ( $J$ ), radical and triplet mutual diffusion coefficient ( $D_r = D_r^R + D_r^T$ ) and triplet zero field splitting (ZFS) parameter,  $D$ . Most treatments of RTPM explain the polarized EPR spectrum by assuming that the doublet levels of the

combined radical-triplet pair are completely quenched, i.e., depleted to the ground state during the encounter (Figure 1A). Very recently, the possibility of inefficient triplet quenching was considered theoretically.<sup>10</sup>

In contrast to RTPM, the triplet in the case of ESPT mechanism is spin polarized during its interaction with the radical, and as of-to-date it was treated only semiempirically.<sup>6,11</sup> Since the triplet ESP (governed by spin lattice relaxation, SLR) precedes the thermal triplet (governed by the triplet decay time to the ground state), a unified treatment of ESPT and RTPM is warranted. In this paper, we present a quantitative treatment of ESPT combined with an extension of the previously reported expressions<sup>7-9</sup> for thermal triplets in RTPM.

An important question regarding the temporal magnetization in triplet-radical interaction process is related to the fate of the triplet following the encounter. Two possibilities should be considered, namely, triplet quenching to the ground-state singlet or triplet survival in the solution. In some of the previous publications an efficient triplet quenching by the radicals was reported,<sup>5,12</sup> while different studies claim that this annihilation

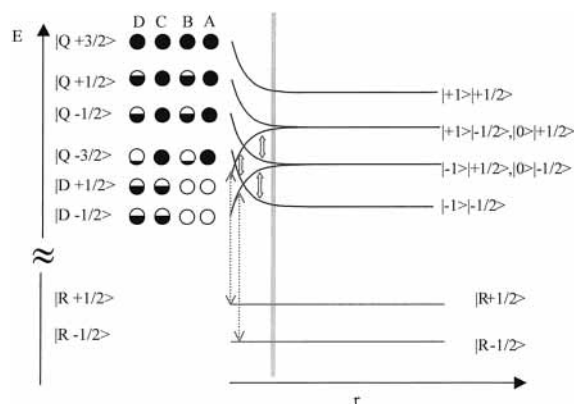


**Figure 1.** Schematic description of RTPM and the energy levels diagram during a triplet-doublet encounter (X-band frequency). Several cases are considered. (A) Triplet encounters a radical, both in Boltzmann population. The excited doublet levels are completely depleted since the transitions,  $|R\pm 1/2\rangle \leftarrow |D\pm 1/2\rangle$  (dotted arrows) are allowed (see text), while the quartet levels have equal population. Notice that a complete depletion of the excited doublet levels leaves two-thirds of the triplet population in tact. (B) The radical encounters a spin-polarized triplet (in emission), with a complete depletion of the doublet levels. (C) Same as case A except that the depletion of the doublet levels is not complete. (D) Same as case C, except that the radical encounters a spin-polarized triplet. The different initial conditions affect the final radical polarization due to different transition efficiencies. Q-D transitions are shown in block arrows). The shadowed region depicts the distance vs energy during the rotational correlation time,  $\tau_c$ , under the condition of  $\tau_c D_i \alpha^2 \ll 1$ .

does not occur efficiently.<sup>6</sup> Other observations suggested that the annihilation occurs only in the RTPM and not in the ESPT processes.<sup>13</sup>

Triplet quenching by free radicals was treated extensively in the last 3 decades,<sup>14-16</sup> including a very recent publication, which discusses this question with relation to RTPM.<sup>10</sup> These theoretical and experimental results, strongly suggest that the quenching rate of the triplet by the radical can be much smaller than diffusion-controlled values. We will address this question of triplet-radical quenching rate by quantitative examination of the radical magnetization in the RTPM process measured in viscous solutions by a pulsed EPR method described recently.<sup>17</sup> The time-resolved EPR (TREPR) results are supported by triplet-triplet optical absorption during triplet-radical encounters. It will be shown that high radical polarization can be generated by RTPM even with inefficient triplet quenching.<sup>18</sup> Finally, an important aspect in describing the radicals' dynamics in the ESPT and RTPM processes mentioned here, is the ability to estimate the triplet-triplet annihilation rate, which is found to be smaller than diffusion-controlled rate.

## II. Experimental Section

Free base tetraphenylporphyrin, H<sub>2</sub>TPP (Aldrich) and its metal substituted ZnTPP (Midcentury Chemical Company), the stable radical  $\alpha,\gamma$ -bisdiphenylene- $\beta$ -phenylallyl, BDPA (Aldrich), were used without further purification (schematically shown in Figure 2). The radical, highly soluble in organic solvents, was chosen due to its narrow line in liquid solution, which makes it suitable for FT-EPR measurements. Dichloromethane and heavy white mineral oil (paraffin oil with viscosity of  $\sim 350$  cP) both of Sigma, were used as solvents. Samples were prepared by dissolving both the BDPA and the porphyrin in dichloromethane and then diluting them in paraffin (20% dichloromethane and 80% paraffin) with a viscosity of  $\sim 25$  cP at 25 °C (measured by comparing the viscosity of the pure paraffin oil to the

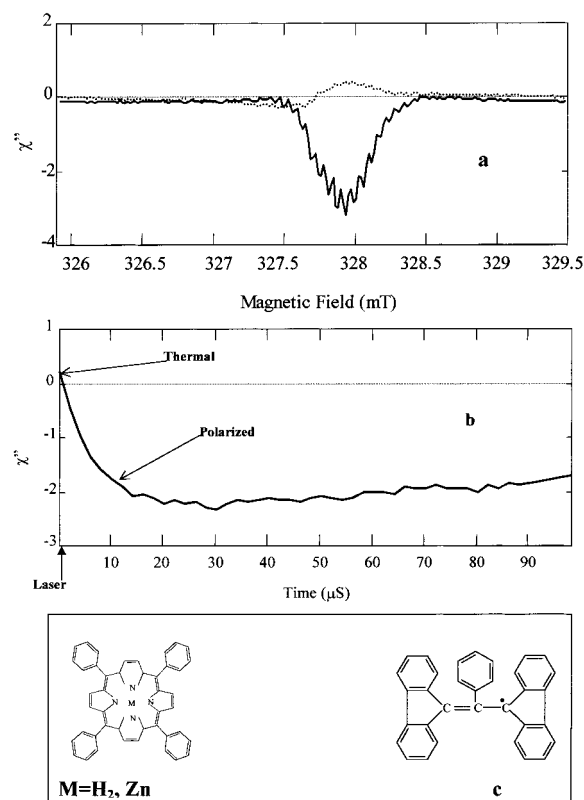


**Figure 2.** FT-EPR spectrum ( $T = 297$  K) of BDPA (with H<sub>2</sub>TPP) before laser excitation (dotted line) and 50  $\mu$ s after the laser excitation (solid line). Notice the hyperfine splitting. (b) Temporal behavior of the magnetization. The arrow indicates the laser pulse excitation at 0.5  $\mu$ s. Notice the negative polarization (emission). The thermal magnetization is measured at the first point of the kinetics curve before the laser pulse. (c) Schematic structures H<sub>2</sub>TPP, ZnTPP, and the radical BDPA.

viscosity of the mixture in a capillary flow measurement). The solutions were inserted in a Pyrex EPR tube (4 mm o.d. and 2.8 mm i.d.) and were sealed under vacuum after several freeze-thaw-pump cycles. FT-EPR measurements were performed with a Bruker ESP 380E spectrometer. The porphyrins in the mixture were photoexcited by a Continuum laser model 661-2D ( $\lambda = 532$ , pulse duration of 12 ns, pulse repetition rate of 20 Hz, and nominal pulse energy of 5 mJ/pulse). At this wavelength the optical absorption of BDPA is negligible. The optimal porphyrin and radical concentrations were found to be  $\sim 5$  and  $\sim 2$  mM, respectively and the initial triplet concentration was calculated to be  $\sim 0.3$  mM, taking into consideration the porphyrin extinction coefficient and light intensity. Under these experimental conditions a considerable dependence of the triplet concentration upon laser light intensity was found. To maximize the experimental effects, the sample size was comparable to the size of the laser light spot ( $\sim 5$  mm). To ensure that there is no sample destruction by undesired photochemical processes, we have considered only results where the radical EPR signal before and after the experiments was the same. Transient absorption measurements were carried out using a 337 nm N<sub>2</sub>-laser (Photronics) (9 ns pulse width) with a dye cell to provide pulses of 0.1 mJ/pulse at 600 nm. The numerical analysis was carried out using Matlab software. All experiments were performed at room temperature.

## III. Results and Discussion

**a. Magnetization Measurements in Viscous Solvents.** ESPT and RTPM in viscous solvents were determined by pulsed-laser

TABLE 1

system <sup>a</sup>	$T_1^R$ (ns)	$T_2^R$ (ns)	$T_1^T$ (ns)	$R_{P,RTPM}$				$R_{P,ESPT}$	
				measured <sup>b</sup>		calcd <sup>c</sup>		measured <sup>d</sup>	calcd <sup>e</sup>
				init	fin	init	fin		
H <sub>2</sub> TPP–BDPA	6900	900	6000	–110	–120	–122	–125	–16	–14
ZnTPP–BDPA	6700	1000	<100 ns	–105	–105	–132	–125		40

<sup>a</sup> Triplet concentration, ~0.3 mM, radical concentration ~2 mM, solvent viscosity ~25 cP. <sup>b</sup> RTPM measurements of radical–polarized triplet interaction (init) and radical–thermal triplet interaction (fin). <sup>c</sup> Calculated values using eqs 10, and 18 with the parameters:  $D = 320$ ,  $J_0 = -16 \times 10^{10}$  rad/s,  $\tau_c = 0.2$  ns,  $D_r = 3.5 \times 10^{-7}$  cm<sup>2</sup>/s, and  $\alpha = 2 \text{ \AA}^{-1}$ . Relative population rates for H<sub>2</sub>TPP were taken as ( $A_x:A_y:A_z$ ): 1.8:0.9:0.3 and for ZnTPP: 0:0:3. <sup>d</sup>  $R_{P,ESPT}$  for ZnTPP could not be measured (see text). <sup>e</sup> Using eq 17.

microwave phase cycling (PLMPC) method described elsewhere.<sup>17</sup> The use of viscous solvents allows to differentiate between ESPT and RTPM, and as will be shown, RTPM increases with viscosity, while ESPT depends very weakly on it.

The PLMPC method is based on two types of pulse sequences. The first sequence is  $\pi/2 - \tau - \text{laser pulse} - \tau_1 - \pi - \tau_1 + \tau - \text{echo detection}$  (fixed  $\tau$  and varied  $\tau_1$ ), which can be described by a vector presentation. The  $\pi/2$  pulse rotates the magnetization (of the radical) into the laboratory  $X$ – $Y$  plane and the rest of the sequence, without the laser pulse, is a simple Hahn echo experiment. The laser pulse applied after the  $\pi/2$  pulse affects only the  $X$ – $Y$  magnetization, without any effects on the  $Z$ -axis magnetization prior to the preparation  $\pi/2$  pulse. It generates the triplets in solution (usually within a time scale of a few nanoseconds), which encounter the stable radicals. Each encounter increases the phase loss of the magnetization in the  $X$ – $Y$  plane and at the same time generates the polarization in the  $Z$ -axis (by the ESPT and RTPM processes). Thus, the encounters reduce the echo amplitude relative to the same sequence when the laser pulse is absent. In cases where the FID overlaps the echo signal, “two element” phase rotation can be used to eliminate the FID signal (Bruker protocol). Analysis of the changes in the echo amplitude as a function of  $\tau_1$ , provides the rate of triplet–radical encounters and their effectiveness, as described recently.<sup>17</sup>

The second sequence is  $\pi/2 - \tau - \text{laser pulse} - 2\tau_1 + \tau - \pi/2 - \text{FID detection}$ , measures the effects related to the magnetization in the  $Z$ -axis. In this sequence the  $Z$ -axis magnetization is detected by the FID at the time of the echo appearance in the first sequence. Again, the preparation  $\pi/2$  pulse flips the entire  $Z$ -axis magnetization, which allows examining only the effects that are related to the generation of  $Z$ -axis magnetization (FID from the second  $\pi/2$  pulse) due to triplet–radical encounters. The combined information gathered by the two sequences, namely triplet–radical encounter rate (first sequence) along with the corresponding  $Z$ -axis magnetization generated by the same encounters (second sequence), provides a direct measurement of the radical polarization. This experimental procedure allows also determining the triplet SLR time via the temporal disappearance of the ESPT polarization in the radical.<sup>17</sup>

A third pulse sequence, consisting of a laser pulse followed by a  $\pi/2$  microwave pulse, was employed to evaluate the total radical magnetization in the time interval 0–100  $\mu$ s after the laser pulse. Such a curve for H<sub>2</sub>TPP–BDPA is shown in Figure 2b. Under these experimental conditions, similar results were obtained for ZnTPP–BDPA system. The strong emissive spectrum due to ESPT and RTPM polarizations is clearly more intense (10-fold) than the thermal one. The quantitative analysis of the temporal magnetization curve (Figure 2b) requires independent evaluation of the triplet SLR time ( $T_1^T$ ) and the radical spin–lattice ( $T_1^R$ ) and spin–spin ( $T_2^R$ ) relaxation times.

The latter values were determined by standard pulse techniques, i.e., three-pulse echo recovery and two-pulse Hahn echo.

**b. Theoretical treatments of ESPT and RTPM.** In many triplet–radical systems, the triplets are polarized before and during the encounter with the radicals.<sup>6,11,13</sup> This phenomena will mainly occur in viscose solutions for triplets of  $D < 500$  G, where the SLR of the triplet is in the order of microseconds,<sup>27</sup> thus affecting the early stages of generated radical polarization. In this section, we will present a general analytical expression valid for ESPT and RTPM, which predict the radical polarization after its encounter with a polarized triplet. While ESPT is treated quantitatively for the first time, the present analysis of RTPM is a generalization based on the treatment presented earlier by Shushin,<sup>7,8</sup> for a triplet whose levels are equally populated. We confine ourselves to the case where the polarization is generated at the vicinity of the crossing regions of the quartet and doublet levels (Figure 1). We shall not consider the case of very high viscosity effect, which was treated in a recent publication.<sup>10</sup> In our treatment, we will derive a closed form expressions, which will provide us with sufficient details to evaluate the influence of triplet ESP on RTPM polarization. For a clear presentation of our findings, we provide the reader with a brief summary of Shushin’s approach on the radical polarization by RTPM.<sup>7,8</sup>

The spin Hamiltonian of the triplet–radical pair is

$$\hat{H} = \hat{H}_z + \hat{H}_{zfs} + \hat{H}_{ex} \quad (1)$$

where

$$\hat{H}_z = \omega_0(\hat{S}_R^z + \hat{S}_T^z) \quad (2)$$

is the Zeeman part ( $\omega_0 = g\beta B_0$ ) assuming the  $g$ -factors of the radical and the triplet are the same.

$$\hat{H}_{zfs} = D\left(\hat{S}_T^2 - \frac{1}{3}\hat{S}_T^2\right) \quad (3)$$

is the ZFS part (assuming  $D \gg E$ ) and  $z$  is the principal axis of the ZFS interaction with the notation that  $X, Y, Z$  and  $x, y, z$  are the laboratory and molecular frames of reference, respectively. All operators are defined in the laboratory frame, and the molecular reorientation in solution results in a time dependent ZFS interaction. The last term of eq 1,

$$\hat{H}_{ex} = -\frac{1}{3}J(r)(1 + 4\hat{S}_R\hat{S}_T) \quad (4)$$

is the exchange interaction, where  $J(r) = J_0 \exp[-\alpha(r - d)]$ , where  $d$  is the distance of closest approach,  $\alpha$  is a scaling parameter, and  $r$  is the distance between the radical and the triplet.

As the triplet and doublet species approach each other, the spin angular momentum is added accordingly.<sup>19</sup> For  $S = S_R + S_T = 3/2$ , the four components of the quartet states are

$$|\hat{Q}_{\pm 1/2}\rangle = \sqrt{2/3}|0\rangle|\pm 1/2\rangle + \sqrt{1/3}|\pm 1\rangle|\mp 1/2\rangle \quad (5a)$$

$$|Q_{\pm 3/2}\rangle = |\pm 1\rangle|\pm 1/2\rangle \quad (5b)$$

And for  $S = 1/2$ , two doublet states are created:

$$|D_{\pm 1/2}\rangle = -\sqrt{1/3}|0\rangle|\pm 1/2\rangle + \sqrt{2/3}|\pm 1\rangle|\mp 1/2\rangle \quad (6)$$

The radical polarization due to triplet–radical encounter is calculated employing the density matrix ( $\rho$ ) in terms of the stochastic Liouville equation:<sup>20</sup>

$$\rho = \hat{L}\rho - i[\hat{H}, \rho] - \hat{W}\rho \quad (7)$$

where the operator  $\hat{L}$

$$\hat{L} = D_r r^{-2} \frac{d}{dr} \left( r^2 \frac{d}{dr} \right) \quad (8)$$

describes the relative diffusion of the triplet–radical pair with a mutual diffusion coefficient  $D_r$ , and the relaxation operator ( $\hat{W}$ ) describes the probabilities of transitions between the spin states of the triplet–radical pair.

In accordance with previous studies,<sup>7</sup> we assume a short rotational correlation time,  $\tau_c$ , of the triplet; namely,  $D\tau_c \ll 1$  and  $D_r\tau_c\alpha^2 \ll 1$  (Table 1). These approximations justify the assumption that the energy difference between the various magnetic levels does not change during  $\tau_c$  (Figure 1). Within the approximation of a short  $\tau_c$ , the transitions between the magnetic levels  $m$  and  $m'$  are<sup>21</sup>

$$W_{mm'} = 2 \overline{|V_{mm'}|^2} \frac{\tau_c}{1 + \omega_{mm'}^2} \quad (9)$$

where  $\omega_{mm'}$  is the splitting between  $m$  and  $m'$  energy levels (in rad/s), and  $V_{mm'} = \langle m|H_{zfs}|m'\rangle$ . With the above definitions and assumptions, it was shown that the radical polarization due to the exchange and the ZFS interactions, after an encounter with a nonpolarized triplet, can be calculated by the equation:<sup>7</sup>

$$R_{P,RTPM} = \frac{d\tau_c}{2D_r\alpha} \sum_{m,m'} \overline{|\langle Q_m|H_{zfs}|D_{m'}\rangle|^2} F(\omega_{mm'}, J_0) \quad (10)$$

Where  $d$  is approximated to be the sum of the radical and triplet radii. The matrix elements, which appear in the summation, represent the ZFS induced quartet-to-doublet transitions (quartet–doublet mixing) averaged over all orientations of the triplet molecule (Figure 1). These elements are calculated to be (neglecting  $E$  in the ZFS Hamiltonian):

$$\overline{|\langle Q_{\pm 3/2}|\hat{H}_{zfs}|D_{\pm 1/2}\rangle|^2} = \frac{1}{3} \overline{|\langle Q_{\pm 1/2}|\hat{H}_{zfs}|D_{\mp 1/2}\rangle|^2} = D^2/45 \quad (11)$$

$$\overline{|\langle Q_{\pm 3/2}|\hat{H}_{zfs}|D_{\pm 1/2}\rangle|^2} = 4D^2/45$$

$F(\omega, J)$  in the summation (eq 10) is<sup>7</sup>

$$F(\omega, J) = \int_0^\infty d\xi \left( \frac{1}{1 + [\omega + 2J e^{-\xi}]^2 \tau_c^2} - \frac{1}{1 + [\omega - 2J e^{-\xi}]^2 \tau_c^2} \right) = \frac{\omega \tau_c}{1 + (\omega \tau_c)^2} \left[ \arctan(\omega - 2J_0) \tau_c - \arctan(\omega + 2J_0) \tau_c + \frac{1}{2\omega \tau_c} \ln \left( \frac{1 + ((\omega - 2J_0) \tau_c)^2}{1 + ((\omega + 2J_0) \tau_c)^2} \right) \right] \quad (12)$$

where  $\omega$  is defined as

$$\omega = \omega_{mm'} = \omega_0 |m - m'| \quad (13)$$

and  $\xi = \alpha(r - d)$ . Equations 10–13 derived by Shushin predicts the radical polarization. This polarization may be positive or negative depending on the sign of  $F(\omega, J)$ .

The structure of eq 10 can be explained qualitatively by assuming that during the encounter, the excited doublet levels are fully depleted (dotted arrows in Figure 1) and the quartet levels remain intact (Figure 1A).<sup>22</sup> This leads to enhanced population transfer from the quartet levels into the empty doublet ones during the time interval between closest approach and separation via diffusion. The transfer rate ( $D \leftarrow Q$ ) is proportional to their respective  $H_{ZFS}$  matrix elements, which induce these transitions (eq 11). The summation in eq 10 consists of three terms; each represents a pair of transitions with a negative and a positive contribution to the radical polarization (eq 11). These plus–minus contributions have equal matrix elements ( $V_{mm'}$ ), but since  $\omega_{mm'}$  are different (Figure 1), the transition probabilities are also different (eq 9). Finally, the integral form of  $F(\omega, J)$  takes care of the fact that the transition rates between the energy levels depend on the varying energy difference  $\omega_{mm'}$  which changes with the separation distance.<sup>7</sup> To summarize, the basic assumption in obtaining eq 10 is that the population of the four quartet states is equal (nonpolarized triplet precursor). Nevertheless, in Shushin's treatment the effect of SLR in the doublet and quartet levels during the encounter was not considered.<sup>23</sup>

We turn now to the case where the radical encounters a polarized triplet, as depicted in Figure 1B. This requires a modification of the original approach,<sup>7,8,12</sup> by taking into account the selective population of the different quartet levels. First, let us examine qualitatively the encounter process, where the wave functions of the triplet and the stable radical are added and result in the quartet and doublet wave functions (eqs 5 and 6 and Figure 1). If the triplet is spin polarized, the excited quartet and doublet states population should reflect it. Also in this case, the excited doublet levels population is negligible due to fast allowed depletion to the ground state (dotted arrows in Figure 1).<sup>22</sup> Upon separation, the quartet polarization is redistributed between the radical and triplet wave functions (treated quantitatively below). Thus, due to strong exchange interaction, which couples the species together and as a result of a polarized triplet precursor, the radicals escaping the cage are generated with a polarization mode (emission or absorption) identical with that of the triplet. This polarization, termed as ESPT,<sup>6</sup> is generated without the involvement of ZFS-induced transitions between the quartet and doublet levels, i.e., ESPT is independent of RTPM.

In the RTPM case, the polarization resulting from the ZFS induced transitions can be calculated quantitatively using eq 10 for thermal triplets. However, for polarized triplets, the initial condition of equal quartet levels population is not valid and eq 10 should be modified. Finally, it should be noted that both

ESPT and RTPM occur simultaneously and result from the same Hamiltonian (eq 1). To treat these processes analytically, it is convenient to discuss them separately. We start with the quantitative description of ESPT.

*i. ESPT.* First, we calculate the polarization, which the radical acquires directly from the triplet. We assume that, during the encounter, the triplet and radical are strongly coupled by the exchange interaction to produce the quartet wave functions (eq 5). Also, we take into account that the polarized triplet is generated by selective triplet  $\leftarrow$  singlet intersystem crossing (ISC) with relative population rates,  $A_x, A_y, A_z$  to the  $x, y, z$  levels in the molecular frame. We can estimate the relative population ( $P_T$ ) of the triplet levels ( $T_0, T_1$ ) in the high-field approximation by the expressions:<sup>24</sup>

$$P_{T_0} = (1/3)(A_x + A_y + A_z) \quad (14a)$$

$$P_{T_{\pm 1}} = P_{T_0} \pm (2/15)(D/B)(A_x + A_y - 2A_z) \quad (14b)$$

Using the quartet wave functions definitions (eq 5), we can calculate the relative population of the quartet levels ( $P_Q$ ), assuming no radical polarization prior to the encounter and negligible triplet SLR:

$$P_{Q_{\pm 3/2}} = P_{T_{\pm 1}} \quad (15a)$$

$$P_{Q_{\pm 1/2}} = 1/3 P_{T_{\pm 1}} + 2/3 P_{T_0} \quad (15b)$$

Thus, when the triplet is polarized, the quartet levels are also polarized and consequently, radical polarization will be developed after separation. The relative population of the radical ( $P_R$ ) after the encounter can be calculated in terms of the radical and triplet wave functions, mixed into the quartet levels (cf. eq 5):

$$P_{R_{+1/2}} = P_{Q_{+3/2}} + 2/3 P_{Q_{+1/2}} + 1/3 P_{Q_{-1/2}} \quad (16a)$$

$$P_{R_{-1/2}} = P_{Q_{-3/2}} + 2/3 P_{Q_{-1/2}} + 1/3 P_{Q_{+1/2}} \quad (16b)$$

Within the scheme of triplet-radical interaction, the radical polarization ( $R_{P,ESPT}$ ) is

$$R_{P,ESPT} = (P_{R_{+1/2}} - P_{R_{-1/2}})/(P_{R_{+1/2}} + P_{R_{-1/2}}) \quad (17a)$$

Which can be expressed in terms of  $A_x, A_y, A_z$ , using eqs 14–16

$$R_{P,ESPT} = (2/9)(D/B)(A_x + A_y - 2A_z)/(A_x + A_y + A_z) \quad (17b)$$

Although eq 17 does not exhibit any explicit time dependence, the actual radical polarization due to ESPT decreases exponentially with  $T_1^T$  toward thermalization (cf. eqs 13 and 18 in ref 17). In addition, ESPT requires the existence of the exchange interaction to couple together the triplet and doublet species. However, since in normal viscosity ( $\eta > 0.1$  cP) the encounter time is much larger than  $J^{-1}$ , eq 17b does not depend explicitly on  $J$ . In other words, the generation of the excited quartet and doublet levels from the triplet and doublet levels is adiabatic, i.e., there is sufficient time available for spin population redistribution among the levels.

*ii. RTPM with a Polarized Triplet Precursor.* Unlike ESPT, RTPM explicitly depends on  $J$ , and the ZFS Hamiltonian. In RTPM, the relevant important factor is  $J/\omega_0$ , whose variation should affect the mixing efficiency and structure of the quartet-

doublet levels (Figure 1). Under these terms of reference, the radical polarization for a polarized triplet precursor is determined by considering eq 10 in which the function  $F(\omega, J)$  is modified into the function  $F'(\omega, J)$ :

$$F'(\omega, J) = \int_0^3 d\xi \left( \frac{P_{Q_-}}{1 + [\omega + 2J_0 e^{-\xi}]^2 \tau_c^2} - \frac{P_{Q_+}}{1 + [\omega - 2J_0 e^{-\xi}]^2 \tau_c^2} \right) \quad (18a)$$

The integral in eq 18a can be solved analytically (Appendix I) and is equal to

$$F'(\omega, J) = \frac{1}{2(1 + \omega^2 \tau_c^2)} (P_{Q_-} \ln W^+ - P_{Q_+} \ln W^-) + \frac{\omega \tau_c}{1 + \omega^2 \tau_c^2} (P_{Q_-} Z^+ + P_{Q_+} Z^-) + 3 \frac{P_{Q_-} - P_{Q_+}}{(1 + \omega^2 \tau_c^2)} \quad (18b)$$

where

$$W^\pm = \frac{1 + \omega^2 \tau_c^2}{1 + \omega^2 \tau_c^2 \pm 4\omega \tau_c^2 J_0 + 4\tau_c^2 J_0^2} \quad (18c)$$

$$Z^\pm = \tan^{-1}(\pm \omega \tau_c) - \tan^{-1}(\pm \omega \tau_c + 2\tau_c J_0) \quad (18d)$$

$P_{Q_+}$  and  $P_{Q_-}$  are the populations of the quartet pairs (eq 15) for the  $m_\pm$  levels, as they appear in eq 11. The final result of the radical polarization is obtained by inserting the modified expression,  $F'(\omega, J)$ , into eq 10. Equation 10 consists of three terms in the summation, which are related to the three pairs of matrix elements in eq 11. Each term requires a different value for  $P_{Q_-}$  and  $P_{Q_+}$  in  $F'(\omega, J)$ : namely,  $P_{Q_{-3/2}}$  with  $P_{Q_{+3/2}}$  for the first term,  $P_{Q_{-1/2}}$  with  $P_{Q_{+1/2}}$  for the second term, and again  $P_{Q_{-3/2}}$  with  $P_{Q_{+3/2}}$  for the third term, each term having a different matrix element. To summarize, eqs 10, 11, 14, 15, and 18, provide the general expression for the RTPM polarization of the radical following an encounter with polarized triplet. However, for most practical cases, two limiting cases are considered, i.e., weak and strong exchange interaction.

*Strong Exchange.* In the strong exchange limit (where  $|J_0| \gg \omega_0 |m - m'| \equiv \omega$  and  $|J_0| \gg 1/\tau_c$ ), eqs 18b and 18c can be approximated to

$$W^\pm = \frac{1 + \omega^2 \tau_c^2}{1 + \omega^2 \tau_c^2 \pm 4\omega \tau_c^2 J_0 + 4\tau_c^2 J_0^2} \approx \frac{1 + \omega^2 \tau_c^2}{1 + 4\tau_c^2 J_0^2} \quad (19a)$$

$$Z^\pm = \tan^{-1}(\pm \omega \tau_c) - \tan^{-1}(\pm \omega \tau_c + 2\tau_c J_0) \approx \tan^{-1}(\pm \omega \tau_c) + \frac{\pi}{2} \text{sign}(J_0) \quad (19b)$$

By plugging eqs 19a and 19b into 18a we obtain

$$F'(\omega, J) = \frac{1}{2(1 + \omega^2 \tau_c^2)} (P_{Q_-} - P_{Q_+}) \ln \left[ \frac{1 + \omega^2 \tau_c^2}{1 + 4\tau_c^2 J_0^2} \right] + \frac{\omega \tau_c}{1 + \omega^2 \tau_c^2} \left\{ (P_{Q_-} - P_{Q_+}) \tan^{-1}(\omega \tau_c) - (P_{Q_-} + P_{Q_+}) \frac{\pi}{2} \text{sign}(J_0) \right\} + 3 \frac{P_{Q_-} - P_{Q_+}}{1 + \omega^2 \tau_c^2} \quad (19c)$$

Inserting eq 19c into eq 10, the final expression is derived for

this limiting case:

$$R_{P,RTPM} = \frac{d \tau_c^2 D^2}{90 D_r \alpha} \left( \frac{1}{2(1 + \omega_0^2 \tau_c^2)} P_1^- \ln \left[ \frac{(1 + \omega_0^2 \tau_c^2)}{(1 + 4\tau_c^2 J_0^2)} \right] + \frac{2}{1 + 4\omega_0^2 \tau_c^2} P_2^- \ln \left[ \frac{(1 + 4\omega_0^2 \tau_c^2)}{(1 + 4\tau_c^2 J_0^2)} \right] + \frac{\omega_0 \tau_c}{1 + \omega_0^2 \tau_c^2} \left[ \tan^{-1}(\omega_0 \tau_c) P_1^- - \frac{\pi}{2} \text{sign}(J_0) P_1^+ \right] + \frac{8\omega_0 \tau_c}{1 + 4\omega_0^2 \tau_c^2} \left[ \tan^{-1}(2\omega_0 \tau_c) P_2^- - \frac{\pi}{2} \text{sign}(J_0) P_2^+ \right] + 3P_2^- \left( \frac{1}{1 + \omega_0^2 \tau_c^2} + \frac{4}{1 + 4\omega_0^2 \tau_c^2} \right) + 3(P_{Q_{-1/2}} - P_{Q_{+1/2}}) \left( \frac{1}{1 + \omega_0^2 \tau_c^2} \right) \right) \quad (20)$$

where

$$P_1^\pm = P_{Q_{-3/2}} \pm P_{Q_{+3/2}} + P_{Q_{-1/2}} \pm P_{Q_{+1/2}}$$

$$P_2^\pm = P_{Q_{-3/2}} \pm P_{Q_{+3/2}}$$

Equation 20 degenerates into that derived previously by Shushin<sup>7</sup> for strong exchange interaction, but with the assumption of equal quartet population (thermal triplet), where  $P_{Q_+} = P_{Q_-} = 1$ .

*Weak Exchange.* In this case,  $|J_0| \ll \omega_0 |m - m'| \equiv \omega$ . Neglecting second-order terms in  $J_0/\omega_0$  (eq 18) and using Taylor expansion, we obtain the following first-order approximations:

$$\ln \left[ \frac{1 + \omega^2 \tau_c^2 + 4\omega \tau_c^2 J_0}{1 + \tau_c^2 \omega^2} \right] \approx \frac{4\omega \tau_c^2 J_0}{1 + \tau_c^2 \omega^2} \quad (21a)$$

$$\tan^{-1}(\omega \tau_c) - \tan^{-1}(\omega \tau_c + 2\tau_c J_0) \approx \frac{-2\tau_c J_0}{1 + \omega^2 \tau_c^2} \quad (21b)$$

Therefore, in the weak exchange approximation  $F'$  (eq 18) is expressed as

$$F'(\omega, J) = - \frac{1}{2(1 + \omega^2 \tau_c^2)(1 + \omega^2 \tau_c^2)} (P_{Q_+} + P_{Q_-}) - \frac{\omega \tau_c}{(1 + \omega^2 \tau_c^2)} \times \frac{2\tau_c J_0}{(1 + \omega^2 \tau_c^2)} (P_{Q_+} + P_{Q_-}) + 3 \frac{P_{Q_-} - P_{Q_+}}{1 + \omega^2 \tau_c^2} = - \frac{4\omega \tau_c^2 J_0}{(1 + \omega^2 \tau_c^2)^2} (P_{Q_+} + P_{Q_-}) + 3 \frac{P_{Q_-} - P_{Q_+}}{1 + \omega^2 \tau_c^2} \quad (22)$$

Plugging eq 22 into eq 10 results in the expression for the radical polarization:

$$R_{P,RTPM} = - \frac{d \tau_c D^2}{90 D_r \alpha} \left\{ - \frac{4\omega_0 \tau_c^2 J_0}{(1 + \omega_0^2 \tau_c^2)^2} P_1^+ + 3 \frac{P_1^-}{1 + \omega_0^2 \tau_c^2} - \frac{32 \omega_0 \tau_c^2 J_0}{(1 + 4\omega_0^2 \tau_c^2)^2} P_2^+ + 3 \frac{P_2^-}{1 + 4\omega_0^2 \tau_c^2} \right\} \quad (23)$$

Again, for  $P_{Q_+} = P_{Q_-} = 1$ , eqs 22 and 23 degenerate into the expressions derived by Shushin.<sup>7</sup> Figure 3 shows the calculated results of the RTPM polarization ( $R_{P,RTPM}$ ) for thermal triplets and for polarized triplets, ESPT polarization ( $R_{P,ESPT}$ ), and the total radical polarization ( $R_{P,ESPT} + R_{P,RTPM}$ ) as a function of viscosity (for ZFS parameter  $D = 330$  G). It can be seen that

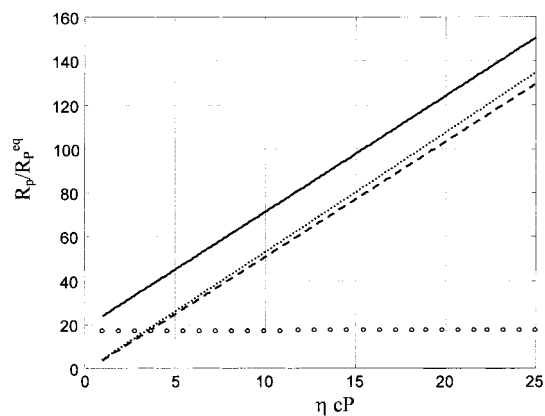


**Figure 3.** Calculated RTPM polarization (normalized to the thermal polarization  $R_p^{eq}$ ) as a function of viscosity with the parameters: triplet ZFS,  $D = 330$  G; triplet radius,  $5 \text{ \AA}$ ;  $J_0 = 16 \times 10^{10} \text{ rad/s}$ ;  $\alpha = 1.4 \text{ \AA}^{-1}$ . The calculation is based on the strong exchange expression (eq 20). The dashed line represents  $R_{P,RTPM}$  only for radical-polarized triplet interaction (cf. Table 1). The dotted line represents  $R_{P,RTPM}$  of the radical after an encounter for radical-nonpolarized triplet interaction. The full circles describe  $R_{P,ESPT}$  (eq 17b). The solid line represents the calculated polarization due to RTPM + ESPT ( $R_{P,RTPM} + R_{P,ESPT}$ ).

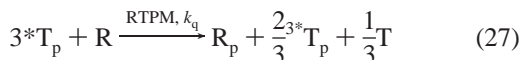
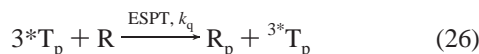
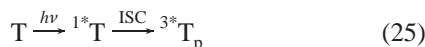
the radical polarization for the unequal quartet levels population, is decreased by about 8% in the RTPM process, relative to its value obtained by assuming equal quartet population. For a larger ZFS parameters, or lower magnetic fields, this difference will increase (for example, for  $D = 1000$  G, at X-band, it will decrease by about 20%). Obviously, the total radical polarization (RTPM + ESPT) will increase.

For the chemical systems we work with,  $J_0$  is in the order of 30 GHz.<sup>17</sup> Therefore, for X-band experiments (10 GHz), the strong exchange limit should be used (eq 20). However, at much higher frequencies (W or D bands, 95 or 130 GHz, respectively) the weak exchange limit should be considered via eq 23. Thus, under the same experimental conditions, such an increase in the microwave frequency will result in decrease in the radical polarization due to RTPM. This can be seen by inspecting the ratio of eq 23 to eq 20, for a simplified cases of  $P_{Q_+} = P_{Q_-} = 1$ , and assuming  $J_0 < 0$ :

$$\frac{R_{P,RTPM}(\text{weak exchange})}{R_{P,RTPM}(\text{strong exchange})} = \frac{4\tau_c J_0 \left[ \frac{1}{(1 + \omega_{02}^2 \tau_c^2)^2} + \frac{8}{(1 + 4\omega_{02}^2 \tau_c^2)^2} \right]}{2\pi \left[ \frac{1}{(1 + \omega_{01}^2 \tau_c^2)} + \frac{8}{(1 + 4\omega_{01}^2 \tau_c^2)} \right]} \quad (24)$$

$\omega_{01}$  corresponds to the lower frequency, where the strong exchange is valid, and  $\omega_{02}$  corresponds to the higher frequency, where the weak exchange is valid. For high viscosity values (in the order of 25 cP, employed in our experiments),  $\tau_c$  is  $\sim 10^{-9}$  s, and  $\omega_{01}\tau_c \geq 1$ , while  $\omega_{02}\tau_c \gg 1$ . Therefore, the ratio of polarizations, which appear in eq 24 is  $\sim [\tau_c J_0 / (\omega_{02}\tau_c)^4] / [1/(\omega_{01}\tau_c)^2] \ll 1$ , i.e., decrease of the polarization at larger Zeeman energies. This prediction of a decrease in the RTPM polarization was recently verified in a high-field experiment, at 130 GHz employing the presently discussed chemical system.<sup>25</sup>

**c. Kinetics of Triplet and Radical Magnetization.** To implement the above considerations on the radical magnetization and the triplet's fate, the following photophysical processes should be considered:<sup>17</sup>



where T stands for the chromophore and the subscript p is the polarization. The processes described by eq 25 are normally very fast and can be considered as instantaneous within the EPR time scale. Equation 26 describes the ESPT interaction (triplet quenching is not required) where the initial triplet polarization is re-distributed between the radical and the triplet. Equation 27 describes the case where a triplet (polarized or nonpolarized) and a stable radical interact through RTPM. Although in the general case, the triplet and the radical can be in any state of polarization, our present treatment considers the interaction of a polarized triplet with a stable nonpolarized radical. As noted in the previous section, ESPT occurs always when a polarized triplet interacts with the radical through the exchange interaction and without triplet quenching. However, RTPM can be “activated” only if at least part of the doublet levels population is quenched during the encounter (Figure 1). This photophysical quenching affects only one-third of the triplet population (cf. eq 27 and case A in Figure 1).

Equations 26–29 can be analyzed by the following coupled differential equations with no microwave power applied:<sup>17</sup>

$$\frac{dM_z}{dt} = \frac{R_{\text{eq}}[R]'}{T_1^R} + k_q f_1 R_p [{}^3T] [R]' \quad (30)$$

$$\frac{d[{}^3T]}{dt} = -\frac{k_q f_2}{3} [{}^3T] [R] - 2k_{TT} [{}^3T]^2 - k_T [{}^3T] \quad (31)$$

where  $M_z$  is the radical magnetization,  $R_p$  is the polarization acquired by the radical in an encounter with a triplet, and  $R_{\text{eq}}$  is the thermal polarization of the radical;  $k_q$  is the triplet-radical diffusion-controlled encounter rate constant,  $f_1$  and  $f_2$  are defined as efficiency factors, which are smaller than 1;  $[{}^3T]$  is the triplet concentration and  $[R]' = [R] \mu_B$ , where  $[R]$  is the radical concentration, and  $\mu_B$  is Bohr magneton;  $k_{TT}$  is the triplet-triplet quenching rate; and  $k_T$  is the triplet decay rate to the ground state;  $T_1^R$  is the radical SLR time. Equations 30–31 can be solved numerically to obtain  $M_z(t)$  expressed by the imaginary susceptibility  $\chi''(t)$ . The calculated  $\chi''(t)$  curves are given in Figure 4 and are based on the measured  $T_1^R$ , the radical and triplet concentration and, since  $R_p$  depends on the triplet SLR, also  $T_1^T$  (given in Table 1). While in  $\text{H}_2\text{TPP-BDPA}$ ,  $T_1^T$  was found to be relatively long (several  $\mu\text{s}$ ), its value in  $\text{ZnTPP-BDPA}$  is very short (less than 100 ns). Thus, within the time resolution of our detection we could observe, in the latter system, radical polarization only due to RTPM. This is consistent with measurements of  $T_1^T$  of  $\text{ZnTPP}$  triplet at room temperature, which is in the order of several tens of ns (Table 1) as compared to much shorter values found at lower temperatures ( $\sim 100$  ns).<sup>17,26</sup> The long  $T_1^T$  of  $\text{H}_2\text{TPP}$  is due to the high viscosity of the solvent, which attenuates the triplet tumbling in solution, thus reducing  $T_1^T$  substantially.<sup>27</sup>

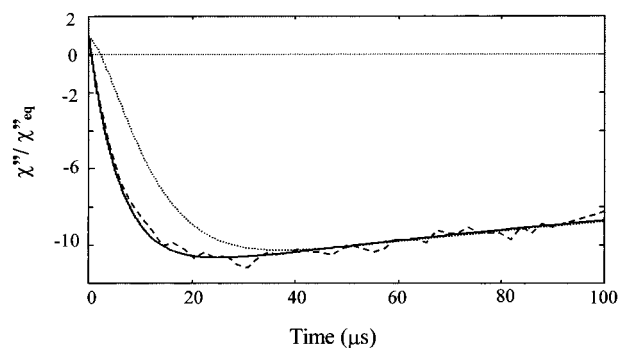


**Figure 4.** Temporal behavior of  $\chi''/\chi'_{\text{eq}}$ . (Dashed) experimental values based upon the magnetization measurements, ( $\text{H}_2\text{TPP-BDPA}$ ); Numerical solution of eqs 30–31 for the two time-dependent polarizations: (dotted) eq 32, (solid) eq 33.

The rate constant  $k_T$  (on the order of  $\sim 100 \text{ s}^{-1}$ )<sup>28</sup> is considered to be negligible for the porphyrins used here. The time dependence of  $R_p$  in eq 30 can be calculated using  $R_{p,\text{ESPT}}$  and  $R_{p,\text{RTPM}}$  values (cf. Table 1). In a recent study, which was based only on experimental measurements of the temporal behavior of the radical polarization, we have shown that the total polarization  $R_p$  can be expressed in terms of the experimental values of  $R_{p,\text{ESPT}}$  and  $R_{p,\text{RTPM}}$  as<sup>17</sup>

$$R_p(t) = R_{p,\text{ESPT}} e^{-t/T_1^T} + (1 - e^{-t/T_1^T}) R_{p,\text{RTPM}} \quad (32)$$

This equation is valid for nonviscous solvents, e.g., toluene, where  $R_{p,\text{RTPM}} \ll R_{p,\text{ESPT}}$  (Figure 3). It indicates that initially ( $t < T_1^T$ ) when the triplet is polarized, the ESPT mechanism is dominant, while later ( $t > T_1^T$ ) RTPM takes over. Inspection of Figure 4, which compares the experimental results to the theoretical predictions, indicates that eq 32 does not meet with the present experimental results, under high viscosity conditions. In other words, when  $R_{p,\text{RTPM}} \ll R_{p,\text{ESPT}}$ , eq 32 cannot describe adequately the experimental curve (Figure 4). Thus, on the basis of our experimental and theoretical analysis, the modified equation should read

$$R_p(t) = R_{p,\text{ESPT}} e^{-t/T_1^T} + R_{p,\text{RTPM}}(t) \quad (33)$$

It is clear that, up to several  $T_1^T$ , these two processes operate simultaneously, and their polarization is added up (cf. Figure 3).

The time dependence of  $R_{p,\text{RTPM}}$  is expressed by eqs 10 and 18. It starts with a radical polarization due to an encounter between a polarized triplet and a stable radical. Later in time, when the triplet is thermalized,  $R_{p,\text{RTPM}}$  converges to the final polarization as calculated by Shushin<sup>7</sup> (eqs 10 and 12). The behavior of  $R_{p,\text{RTPM}}$  can be also described by inspection of Figure 1 (Cases A and B). The first case relates to the initial condition where all four quartet levels are equally populated. In this case, the radical polarization  $R_{p,\text{RTPM}}$  is mainly due to transitions  $D_{\pm 1/2} \leftarrow Q_{-3/2}$  and  $D_{+1/2} \leftarrow Q_{-1/2}$  (expressed by the block arrows in Figure 1). Figure 1B describes the levels population when the radical encounters a polarized triplet. In the case of a net emission mode as in  ${}^3\text{H}_2\text{TPP}$ ,<sup>28</sup>  $Q_{-3/2}$  and  $Q_{-1/2}$  are less populated than in the first case, and  $|R_{p,\text{RTPM}}|$  will be smaller. Nevertheless, the total polarization of the radical, expressed by eq 33 and in Figure 3, increases. The opposite holds for an encounter of a polarized triplet in enhanced absorption mode, e.g.,  ${}^3\text{ZnTPP}$ .<sup>28</sup>

The numerical solution of eqs 30–31 (Figure 4) provides the value of  $k_{TT}$  which is  $6.5 \times 10^6 \text{ M}^{-1} \text{ s}^{-1}$ , namely,  $\sim 40$  times

smaller than the diffusion-controlled rate,  $k_q = 2.6 \times 10^8$ .  $k_q$  was calculated using the estimated radius of the excited triplet molecule (5 Å) and solvent viscosity (25 cP) via the equation

$$k_q = 4\pi (R_T + R_R)(D_T + D_R)N_A \quad (34)$$

where  $R_T$  and  $R_R$  are the triplet and radical radii, respectively,  $D_T$  and  $D_R$  are the diffusion coefficients of the triplet and radical, respectively, and  $N_A$  is Avogadro's number. The experimental curve in Figure 4 can be simulated by considering an efficiency factor  $f_1 = 1/4$  (eq 30), for the RTPM process and a partial quenching of the triplet by the radical with efficiency factor  $f_2 = 1/40$  (eq 31). Thus, it is concluded that the quenching of the triplet by the radical is much smaller than the diffusion-controlled value,  $k_q$ . This case is depicted in Figure 1C,D. The factors  $f_1$  and  $f_2$  are not equal since they relate to different processes, i.e., radical polarization and triplet quenching, respectively. However, for the case where RTPM is dominant,  $f_1$  and  $f_2$  are closely related. For example, a small quenching efficiency, i.e.,  $f_2$ , will result in inefficient generation of radical polarization (i.e., small  $f_1$ ).<sup>10</sup>

Further justification for the small value of  $f_2$  can be made by the following theoretical argument. Triplet quenching during triplet-doublet encounter can occur by two main mechanisms: (1) Energy transfer from the excited triplet level to the excited doublet level<sup>16</sup> and (2)  $S_0 \leftarrow T_1$  enhanced ISC, due to the triplet interaction with the doublet.<sup>14,15</sup> Since at 532 nm the optical absorption of BDPA radicals is negligible, it is reasonable to assume that the energy levels of the triplets are lower than the first excited doublet level of BDPA. Thus, we can safely rule out the former mechanism and consider only the latter one. The rate of the enhanced ISC can be estimated from the equation<sup>14,15</sup>

$$k_{ISC} = \frac{2\pi |H_{ex}|^2 F}{\hbar H_v} \quad (35)$$

where  $H_{ex}$  is the exchange interaction matrix element during the encounter,  $F$  is the Franck-Condon factor, and  $H_v^{-1}$  is the density of the final vibrational energy states (after quenching). For aromatic hydrocarbons  $F$  is expressed by<sup>29</sup>

$$F = 0.15 \times e^{\{-(\Delta E - 4000)/2175\}} \quad (36)$$

where  $\Delta E$  the energy (in  $\text{cm}^{-1}$ ) between the triplet and singlet ground state. Assuming an efficient coupling between the vibrational states and the bulk, a lower limit for the internal conversion rate is  $\sim 10^{12} \text{ s}^{-1}$ , which corresponds to  $H_v \sim 30 \text{ cm}^{-1}$ . Typical  $\Delta E$  for porphyrins are  $\sim 12\,000 \text{ cm}^{-1}$  and the exchange interaction during the encounter was estimated to be  $\sim 1 \text{ cm}^{-1}$ .<sup>17</sup> Inserting these values in eq 35 results in a value of  $k_{ISC} \sim 2 \times 10^7 \text{ s}^{-1}$ . Mutual diffusion coefficient,  $D_r$  (in  $\text{cm}^2/\text{s}$ ), of the triplet and radical can be estimated through the Stokes-Einstein relation:

$$D_r = D_T + D_R = \frac{100k_B T}{6\pi\eta} \left( \frac{1}{R_T} + \frac{1}{R_R} \right) \quad (37)$$

where  $k_B T$  (in erg),  $\eta$  (in cP), and  $R_T$  and  $R_R$  (in cm) represent the radius of the triplet and radical, respectively. Thus, the encounter time can be estimated from the relation:<sup>30</sup>

$$\tau \approx \frac{(R_e)^2}{D_r} \quad (38)$$

where  $R_e$  is the distance and where  $J$  is operational and estimated

to be  $\sim 2 \text{ \AA}$ .<sup>17</sup> Thus, with a solvent viscosity of 25 cP, the encounter time  $\tau$  is calculated to be  $\sim 2 \times 10^{-8} \text{ s}$ , i.e.,  $k_{ISC}\tau \approx 1$ , implying that the triplet quenching is inefficient, in line with our results.<sup>30,31</sup>

Finally, it should be noted that in previous reported studies, the case of inefficient triplet quenching was not considered theoretically<sup>7</sup> nor observed experimentally.<sup>5,12</sup> The systems investigated in the early studies are those where the triplet state lie above that of the excited doublet.<sup>18</sup> In these cases, energy transfer mechanism is more probable, thus resulting in an efficient triplet quenching by the radical.

#### IV. Conclusions

We have extended the previous findings concerning the interaction of stable radicals with photoexcited triplets. With respect to ESPT, which is relevant only when the radical encounters a polarized triplet, a quantitative treatment predicts the radical polarization in the encounter. In the RTPM case, while the existing studies were restricted to radicals interacting with thermal triplets, the present study provides a general solution where the radicals can interact with polarized and nonpolarized triplet (generalized RTPM). An important feature of RTPM is associated with the efficiency of triplet quenching during the encounter process. By acquiring accurate polarization measurements together with quantitative magnetization results, we have shown that the quenching efficiency can be estimated. The relatively low efficiency of the triplet quenching accompanied by relatively high RTPM efficiency is unique to the porphyrin systems. It is due to the fact that the porphyrins have relatively low triplet energy.

#### V. Acknowledgment.

This work is in partial fulfillment of the requirements for a Ph.D. degree (A.B.) at the Hebrew University of Jerusalem. This work was partially supported by the Israel Ministry of Science, through the "Eshkol Foundation Stipends" (A.B.), and by a US-Israel BSF grant and by the Volkswagen Foundation (I/73 145). The Farkas Research Center is supported by the Bundesministerium für die Forschung und Technologie and the Minerva Gesellschaft für Forschung GmbH, FRG. We appreciate the help of David Ovrutsky and Prof. Michael Ottolenghi in performing laser photolysis experiments.

#### VI. Appendix I

The indefinite integral in the function  $F(\omega, J)$  in eq 12 has the analytical solution:

$$\int d\xi \left( \frac{1}{1 + [\omega \pm 2J e^{-\xi}]^2 \tau_c^2} \right) = \frac{1}{2(1 + \omega^2 \tau_c^2)} \ln[1 + \omega^2 \tau_c^2 \pm 4\omega \tau_c^2 J_0 e^{-\xi} + 4\tau_c^2 J_0^2 e^{-2\xi}] \pm \frac{\omega \tau_c}{1 + \omega^2 \tau_c^2} \tan^{-1}[\pm \omega \tau_c + 2\tau_c J_0 e^{-\xi}] + \frac{\xi}{1 + \omega^2 \tau_c^2} \quad (A1)$$

We integrate this function over the interval  $\xi = 0-3$ , which corresponds to a radial-triplet distance from  $d$  to  $d+3/\alpha$  (10 Å to 11.5 Å in the triplet-radical systems we employed). This is a realistic distance for the induced ZFS  $D \leftarrow Q$  transitions, when the exchange interaction is not zero. The infinite boundaries, as in eq 12 cannot be used due to the divergence of the integral, which is not avoided if  $P_{Q+}$  is not equal to  $P_Q$ . After the integration we obtain



$$\int_0^3 d\xi \left( \frac{1}{1 + [\omega \pm 2J_0 e^{-\xi}]^2 \tau_c^2} \right) = \frac{1}{2} \frac{1}{1 + \omega^2 \tau_c^2} \ln \left[ \frac{1 + \omega^2 \tau_c^2 \pm 4\omega \tau_c^2 J_0 e^{-3} + 4\tau_c^2 J_0^2 e^{-6}}{1 + \omega^2 \tau_c^2 \pm 4\omega \tau_c^2 J_0 + 4\tau_c^2 J_0^2} \right] \pm \frac{\omega \tau_c}{1 + \omega^2 \tau_c^2} \{ \tan^{-1} [ \pm \omega \tau_c + 2\tau_c J_0 e^{-3} ] - \tan^{-1} [ \pm \omega \tau_c + 2\tau_c J_0 ] \} + \frac{3}{1 + \omega^2 \tau_c^2} \quad (\text{A2})$$

By neglecting the terms multiplied by  $e^{-3}$  and  $e^{-6}$ , we obtain eq 18. It should be noted that more accurate treatment of the crossing regions problem, considered recently,<sup>10</sup> will lead to an effective truncation of the integral at the boundary of the approaching regions. However, using an upper, limit of 3 in our case, provides a simple method of avoiding divergence of the solution.

## References and Notes

- Thurnauer, M. C.; Meisel, D. *Chem Phys Lett.* **1982**, *92*, 343.
- Blättler, C.; Jent, F.; Paul, H. *Chem. Phys. Lett.* **1990**, *166*, 375.
- Kawai, A.; Obi, K. *J. Phys. Chem. A* **1992**, *96*, 5701.
- Kawai, A.; Obi, K. *Res. Chem. Intermed.* **1993**, *19*, 865.
- Kobori, Y.; Takeda, K.; Tsuji, K.; Kawai, A.; Obi, K. *J. Phys. Chem. A* **1998**, *102*, 5160.
- Fujisawa, J. I.; Ohba, Y.; Yamauchi, S. *J. Phys. Chem. A* **1997**, *434*.
- Shushin, A. I. *Chem. Phys. Lett.* **1993**, *208*, 173.
- Shushin, A. I. *J. Chem. Phys.* **1993**, *99*, 8723.
- Adrian, F. J. *Chem. Phys. Lett.* **1994**, *229*, 465.
- Shushin, A. I. *Chem. Phys. Lett.* **1999**, *313*, 246.
- Fujisawa, J.; Ohba, Y.; Yamauchi, S. *Chem. Phys. Lett.* **1998**, *294*, 248.
- Goudsmit, G.-H.; Paul, H.; Shushin, A. I. *J. Phys. Chem. A* **1993**, *97*, 13243.
- Saiful, I. S. M.; Fujisawa, J.; Kobayashi, N.; Ohba, Y.; Yamauchi, S. *Bull. Chem. Soc. Jpn.* **1999**, *72*, 661.
- Hoytink, G. J. *Acc. Chem. Res.* **1969**, *2*, 114
- Gijzeman, O. L. J.; Kaufman, F.; Porter, G. *J. Chem. Soc., Faraday Trans. II* **1973**, *95*, 9130.
- Kuzmin, V. A.; Tatikolov, A. S. *Chem. Phys. Lett.* **1978**, *53*, 606.
- Blank, A.; Levanon, H. *J. Phys. Chem. A* **2000**, *104*, 794.
- The effectiveness of triplet quenching can be explained by the relative location of the triplet energy levels,  ${}^3E_T$  relative to the radical excited states of the doublet  ${}^*E_R$ . When  ${}^3E_T > {}^*E_R$ , the triplet can be quenched through energy transfer mechanism, whereas for  ${}^3E_T < {}^*E_R$  the triplet quenching by this mechanism is much less effective.
- Weil, J. A.; Bolton, J. R.; Wertz, J. E. *Electron Paramagnetic Resonance*, Wiley: New York, 1994; p 439.
- Kubo, R. *Adv. Chem. Phys.* **1969**, *16*, 101.
- Abraham, A. *The Principles of Magnetic Resonance*; Oxford University Press, New York, 1961; p 264.
- Nakvi, R. K. *J. Phys. Chem.* **1981**, *85*, 2302.
- We look at a typical "in-cage lifetime" of the neutral triplet-radical pair,  $\tau = d^2/D_r$ .<sup>30</sup> Neglecting the SLR is justified for  $\tau \ll T_1^T$ . Since  $T_1^T$  depends strongly on the ZFS parameter,  $D$ ,<sup>27</sup> then for  $D < 500$  G,  $T_1^T > 10$  ns, in nonviscous solvents ( $\eta \sim 1$  cP), while  $\tau \ll 1$  ns. For such triplets, neglecting SLR during the encounter is justified. However, for  $D > 500$  G,  $T_1^T$  cannot be ignored. In our case,  $D \sim 400$  G and  $T_1^T$  during the encounter can be safely neglected.
- Wong, S. K.; Hutchinson, D. A.; Wan, J. K. S. *J. Chem. Phys.* **1973**, *58*, 985.
- We are grateful to Dr. O. Poluektov, and Dr. M. C. Thurnauer, for running the preliminary experiments at 130 GHz.
- Yamauchi, S. Private communications.
- Atkins, P. W.; Evans, G. T. *Mol. Phys.* **1974**, *27*, 1633.
- Gonen, O.; Levanon, H. *J. Chem. Phys.* **1983**, *78*, 2214.
- Siebrand, W. *J. Chem. Phys.* **1967**, *46*, 2411.
- Salikhov, K. M.; Molin, Y. N.; Segdeev, R. Z.; Buchachenko, A. L. *Spin Polarization and Magnetic Effects in Radical Reactions*; Elsevier: Amsterdam, 1984; p 56.
- Supporting evidence to the above conclusion is given by triplet-triplet optical absorption measurements. The triplet decay rate was determined with the presence and absence of the free radical. The results reconfirm our findings that even high radical concentration does not affect substantially the triplet lifetime.